L-7810

ANL-7810

DEVELOPMENT OF A MIXER-SETTLER FOR LIQUID METAL-SALT SYSTEMS

J. B. Knighton, G. J. Bernstein,
G. N. Vargo, and R. D. Pierce

U of C-AUA-USAEC

ARGONNE NATIONAL LABORATORY, ARGONNE, ILLINOIS

Printed in the United States of America
Available from
National Technical Information Service
U.S. Department of Commerce
5285 Port Royal Road
Springfield, Virginia 22151
Price: Printed Copy $3.00; Microfiche $0.95

ANL-7810
Chemical Separations Processes
for Plutonium and Uranium

ARGONNE NATIONAL LABORATORY
9700 South Cass Avenue
Argonne, Illinois 60439

DEVELOPMENT OF A MIXER-SETTLER FOR LIQUID METAL-SALT SYSTEMS

by

J. B. Knighton, G. J. Bernstein,
G. N. Vargo, and R. D. Pierce

Chemical Engineering Division

June 1971

TABLE OF CONTENTS

LIST OF FIGURES

LIST OF FIGURES

LIST OF TABLES

DEVELOPMENT OF A MIXER-SETTLER FOR LIQUID METAL-SALT SYSTEMS

by

J. B. Knighton, G. J. Bernstein, G. N. Vargo,
and R. D. Pierce

ABSTRACT

A single-stage mixer-settler has been developed for application in a multistage extraction process to extract plutonium from spent LMFBR fuel material. This device is designed to separate plutonium from fission products by salt extraction and salt transport procedures. (Salt transport is selective transfer of a solute from a liquid donor alloy to a liquid acceptor alloy by circulating molten salt between the two alloys.) The design of the unit fabricated here provides for contacting of two liquid phases in a mixing chamber by blades on the outside of a hollow agitator-pump rotating in the mixing chamber; the mixture is then pumped through the interior of the mixer-pump to discharge openings at its top, from which the mixture is routed as required for a particular application.

Preliminary tests with a 5-cm OD, 20-cm long stainless steel mixer-pump showed it to be capable of pumping Mg-Cu alloy at 670°C. However, mixing blades at the bottom of the mixer-pump failed to provide sufficient agitation.

A second stainless steel mixer-pump was fabricated. This pump employed a stepped cylindrical wall with mixing blades attached to the outer surface of the pump near its bottom. A mixing chamber design was developed whereby gas entrainment in the mixing chamber was eliminated. In runs with water only, flow rate was related to pump speed, the size of the inlet orifice in the bottom of the pump, and the depth of water on the outside of the pump (pump submergence). The residence time distribution for water flowing through the mixing chamber was also studied. High temperature runs were performed with the mixer-pump installed in an assembly containing a settling chamber, all within a sealed heated vessel. Metal flow rates were successfully measured with a metering cup and an induction liquid-level probe. To measure extraction efficiency, tagged cerium was extracted from Mg-Cu alloy into chloride salts at 650°C. Stage efficiencies above 99% were achieved. The overall mechanical performance of the single-stage mixer-settler is considered satisfactory.

I. INTRODUCTION

The Salt Transport Process previously under development at Argonne (Appendix A) incorporates multistage liquid metal-molten salt extraction steps for the purification of plutonium and uranium from spent LMFBR fuels.[1] In salt transport, a solute is transferred selectively from a liquid donor alloy to a liquid acceptor alloy by circulating a molten salt between the two alloys. The chemical basis of salt transport separation is presented in Appendix B. For this work, the starting material for the Salt Transport Process was assumed to be stainless steel-clad UO_2-PuO_2, which is the probable fuel for the first commercial LMFBR's.

The initial steps of this process are decladding and oxide reduction steps in which many of the fission products and most of the uranium are separated from plutonium. At the end of the reduction step, the plutonium is in solution in a liquid Mg-Cu alloy along with some fission products and excess calcium reductant; the uranium, which has a solubility of about 50 ppm in the alloy, forms a bed of precipitated metal.

Requirements for the plutonium extraction steps that follow reduction are recovery of 99.8% of the plutonium and a decontamination factor of 10^6 for fission product radioactivity. The plutonium must be separated from yttrium, the rare earth elements, nobler fission elements (zirconium, niobium, ruthenium, molybdenum, technetium, and palladium), and small quantities of uranium and stainless steel cladding elements (iron, chromium, and nickel). As is described in detail in Appendix C, separation of plutonium from impurities is accomplished by (1) selective extraction of yttrium and the rare earths from the Mg-Cu-Pu alloy into a molten chloride salt, (2) selective extraction of plutonium from the alloy into another chloride salt stream, and (3) extraction of the purified plutonium from the salt into Zn-Mg alloy to obtain plutonium in concentrated form. Neptunium and curium follow plutonium through the extraction, but the other transuranium elements are removed when the rare earths are extracted. Another requirement in the plutonium extraction steps is that the volumes of waste streams be small but not so small that removal of decay heat is a problem.

The selection of an extraction philosophy for the Salt Transport Process required consideration of the following factors: specifications for product and wastes, plutonium inventory, criticality restrictions, waste volumes, materials of construction, process control, process flexibility, and phase transfer efficiency.

To achieve the desired high plutonium decontamination and recovery, multistage extraction is necessary. Batchwise operation was rejected for multistage extraction because of the many phase transfers that would be involved and because of the difficulty of performing the clean phase separations necessary to utilize the large separation factors available. Countercurrent columns were considered for the process[2] but were not selected for the current flowsheet because they are not compatible with the flow pattern selected. A semicontinuous salt transport procedure employing a battery of mixer-settlers was adopted. A variety of flow patterns of heavy and light phases may be employed with this equipment.

Mixer-settler designs used in the chemical processing industry were reviewed.[3-8] Probably the simplest and most versatile form is one in which mixing is done in one vessel and settling in another. In a conventional multistage mixer-settler, two liquids flow continuously and countercurrently through the stages. In the proposed seven-stage mixer-settler for plutonium purification, two salt streams and three metal streams are employed. The unconventional flow patterns in the present process eliminated some designs. Some mixer-settler designs were eliminated from consideration because of the elevated temperature of operation for this pyrochemical process and limitations in fabrication of suitable materials of construction.

A box-type mixer-settler was selected as the most appropriate for this study. The components of this mixer-settler are (1) a mixer that consists of a hollow cylindrical mixer-pump that partially extends into a mixing chamber and (2) a settler (settling chamber). In the operation of a mixer-settler, two liquid streams are fed into the mixing chamber, where they are contacted by blades on the outside wall of the rotating mixer-pump, effecting the extraction of a solute from one stream into the other. The mixture enters the bottom of the mixer-pump through an orifice located at the axis of the mixer-pump. The action of liquid inside the mixer-pump is similar to that in a vertical-bowl centrifuge. Centrifugal pressure forces a column of liquid up the inside wall of the rotating cylinder until the pressure due to the column of liquid equals the centrifugal pressure of the rotating liquid. The head that develops is proportional to the square of the rotational speed and to the difference between the square of the internal radius of the pump tube and the square of the radius of the inlet:

$$h_\ell \rho g = \frac{\rho \omega^2}{2} (r_2^2 - r_1^2)$$

where h_ℓ is the height of liquid lift, g is the acceleration of gravity, ω is the speed of rotation, r_1 is the radius of the orifice, and r_2 the radius of the rotating cylinder. Since ρ, the liquid density, cancels out

$$h_\ell = \frac{\omega^2}{2g} (r_2^2 - r_1^2)$$

and h_ℓ is dependent only on ω, g, r_1, and r_2. The total lift available is the sum of the head developed by the pump and the inlet pressure inside the orifice. The pumping rate is a function of the excess head developed by the pump and may also be limited by the size of the orifice. The mixture flows into a collection chamber at the top of the mixer-pump and then into a settling chamber. The liquid is pumped to a high enough elevation to allow gravity feeding to the next step.

Because of the special fluid movement requirements, this extractor concept was chosen in which a positive pumping action was provided rather than employing the head developed by the agitator blades to assist gravity flow as in other mixer-settler designs.[3,6] Similar pumps without mixing blades are used for batch transfer of fluid from the settling region of one stage to the settling region of an adjoining stage. The proposed flow patterns are shown in plan view in Fig. 1.

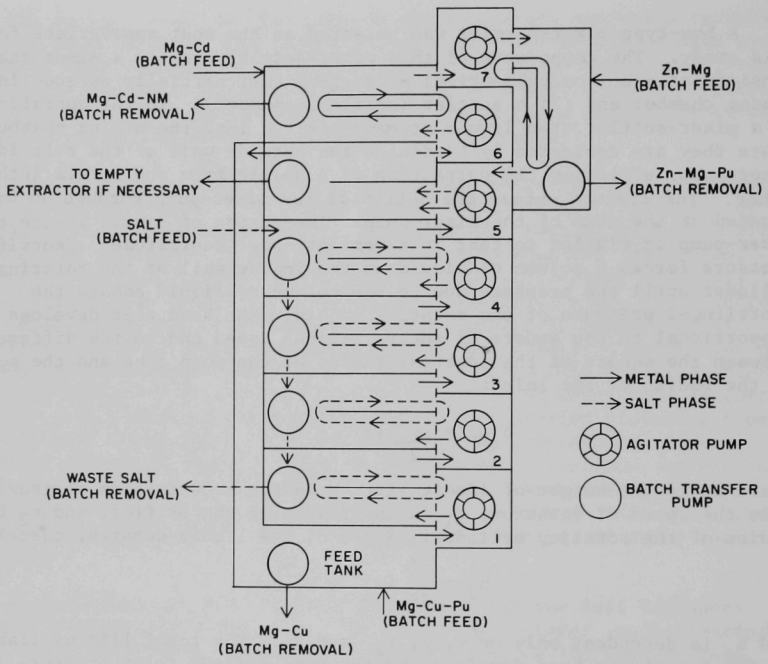

Fig. 1. Seven-Stage Mixer-Settler - Schematic Plan View.
ANL Neg. No. 308-1882.

To simplify the design and fabrication of the mixer-settlers, a modular concept was employed in which the mixing chambers, settlers, and mixer-pumps for all stages are similar. Thus, only one mixer-settler and mixer-pump configuration had to be studied. Each mixing chamber and each settler is a separate vessel and are assembled in a common furnace to form a seven-stage mixer-settler.

The objective of these studies was to establish a mixer-pump and mixing chamber design by fabricating an acceptable single-stage mixer-settler that can be operated with either the salt phase or the metal phase captive. This report gives the status of development of mixer-settler equipment for the plutonium purification step. Preliminary experiments utilized a plastic mixer-pump. In other initial experiments, a stainless steel mixer-pump of preliminary design was operated in a furnace to study its capability of pumping molten metal. The final mixer-pump, fabricated of stainless steel, was operated in a plastic mixing chamber with water during development of the mixing chamber design and study of variables affecting mixing power, pumping rate, and residence time. This same mixer-pump was later operated in a furnace at 650°C to measure stage efficiency in runs in which tagged cerium was extracted from Mg-Cu alloy into molten salts.

At the stage of equipment development reported here, the Salt Transport Process program was terminated because of budgetary limitations.

II. DESIGN AND EVALUATION OF MIXER-PUMPS

In the development of a single-stage mixer-settler, the initial mixer-pumps were built of plastic, permitting visual observation. A mixer-pump rotating inside a square mixing chamber was selected for development because of its simplicity. The mixer-pump was a rotating hollow cylinder but need not have been cylindrical; a conical shape[a] would be desirable.

Early in the mixer-settler development program, a mixer-pump was built that could be operated with molten Mg-Cu alloy. This 5.1-cm OD, 20-cm-long cylindrical mixer-pump, which was employed for the preliminary studies with water-organic systems and with Mg-Cu alloy, had small mixer blades attached to the bottom surface.

The mixer-pump components (Fig. 2) were fabricated of type 304 stainless steel. From left to right are a displacement tank for adjusting the depth of the Mg-Cu alloy in the alloy sump, the mixer-pump, mixing and collection chambers, a metering cup for flow rate determination, and a vessel to contain the other components and to serve as a sump for the Mg-Cu alloy. The assembled components are shown in Fig. 3. In this photograph, the pump rests on the bottom of the mixing chamber.

---

[a] A plastic conical pump performed in an excellent manner with a minimum of fluid holdup in the pump, but the conical pump was not developed further because fabrication using a material suitable for the process fluids would be expensive.

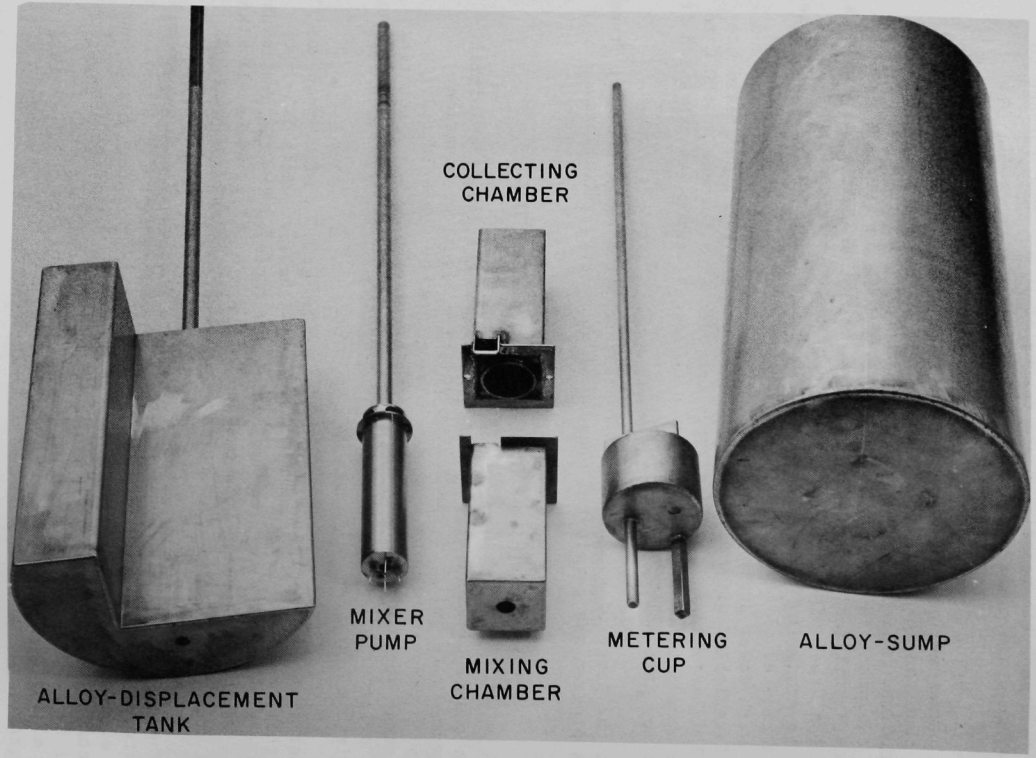

Fig. 2. Components for Molten Alloy Mixer-Pump Tests.
ANL Neg. No. 308-1659A.

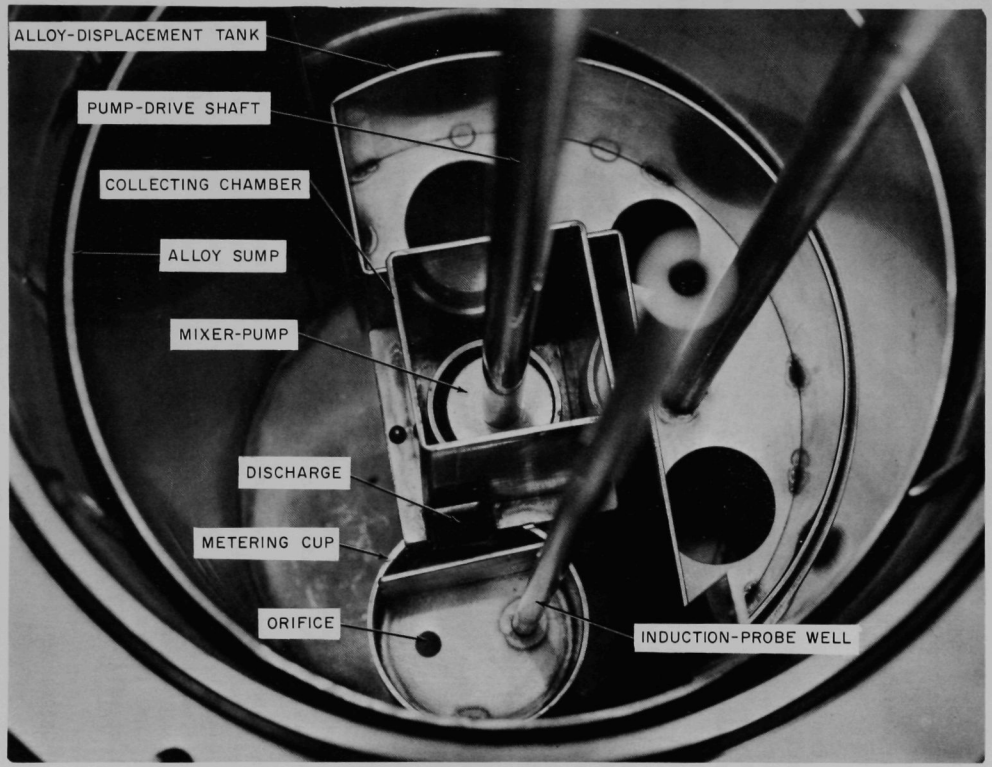

Fig. 3. Top View of Assembly for Molten Alloy Mixer-Pump Tests. ANL Neg. No. 308-1652A.

In operation, the pump was raised so that it discharged into the collection chamber. The liquid alloy flowed from the collection chamber to the metering cup and then through an orifice in the bottom of the metering cup back to the sump. The level of liquid in the metering cup was determined with a mutual inductance probe[9] inserted in a well that extends through the cup. The metering cup was calibrated by (1) filling the metering cup to overflowing with alloy by pumping at a high rate, (2) stopping the pump, and (3) recording the induction probe readings as a function of time as the cup emptied. The results, expressed as volume of fluid in the cup versus time, were fitted to a quadratic equation by least squaring. This function was differentiated to determine the flow rate corresponding to any depth of fluid in the cup.

A tracing of a typical meter cup decay curve is presented in Fig. 4. The chart reading of the induction probe signal for an empty cup differed from the reading for an overflowing cup by 2.9 mV. A hysteresis effect was noted--an extended period was required before a zero reading was re-established. This effect has been attributed to metal clinging to the probe well and to the cup bottom. Note that late in the drainage curve the chart was stopped for several minutes. The portion of these data for 1.5 to 17 sec after the pump was stopped was used to determine the calibration curve. During a seven-day period while the pump assembly was held in a furnace at a temperature of 670°C, the pump was operated for 55 hr at submergences in Mg-Cu alloy ranging from 2.4 to 6 cm and at speeds ranging from 860 to 1050 rpm. The flow rates obtained at given submergences were measured. Results agreed well with data obtained earlier when a mixture of water and acetylene tetrabromide was pumped with the same pump. The two sets of data for a pump speed of 1000 rpm are compared in Fig. 5. These comparisons show that pumps suitable for high-temperature operation can be calibrated with aqueous-organic systems.

Studies using water-organic systems, with the mixer-pump installed in a plastic mixing chamber, showed that the mixing blades on this pump failed to provide sufficient agitation. Also, the centrifugal pumping action of the blades decreased the inlet pressure at the pump orifice; therefore, a greater speed was required to force the liquid to the top of the pump.

Throughout the high temperature Mg-Cu alloy run, problems were encountered with bearings and shaft run-out. Oil-impregnated bearings failed rapidly, but ball bearings performed satisfactorily. Because of excessive shaft run-out, the pump and the collecting ring rubbed and were scored. These mechanical difficulties were corrected for the mixer-settler unit (described in the following section) that was used to study extraction efficiency.

III. DESIGN AND INVESTIGATION OF MECHANICAL OPERATION AND EXTRACTION EFFICIENCY OF MIXER-SETTLER

A single-stage mixer-settler was designed and fabricated for use in determining extraction efficiencies and investigating the mechanical operation of the apparatus. A stepped cylindrical mixer-pump was employed. Its cylinder had a 4.8-cm ID in the submerged mixing region to provide a larger mixing zone and to allow room for mixing blades which were mounted

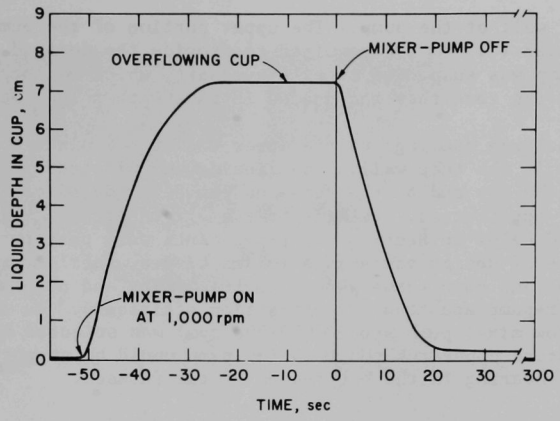

Fig. 4. Metering-Cup Decay Curve

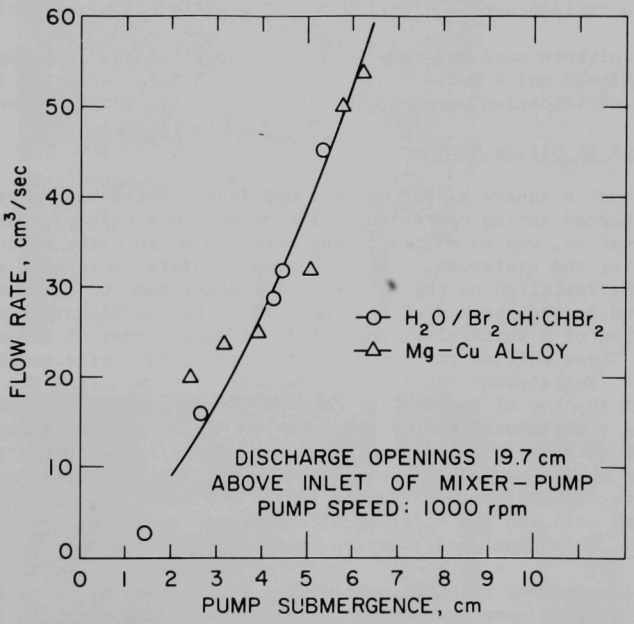

Fig. 5. Effect of Pump Submergence on Output of 5-cm dia Mixer-Pump

on the outer wall of the pump. The upper portion of the pump had the larger diameter (7.3-cm ID) required to provide the desired pumping rate. The mixer-pump was suspended on a heavy shaft, which was supported and sealed above the zone that was heated in runs with molten metal-salt.

The discharge openings at the upper end of the mixer-pump consisted of slots cut in the tube wall. The liquid was collected in a chamber surrounding the top end of the tube and could be routed as required for a particular application. Details of the mixer-settler design and operation are presented below in Section D. Experiments were performed to observe the influence of design variations (mixer blades, baffles, speed of rotation, orifice size, and pump submergence) on the mixing and pumping characteristics of this mixer-pump and to study extraction efficiency. In this work, a relatively low mixer-pump speed (600-900 rpm) was selected because in the high temperature apparatus the rotating pump would be supported at only one end, with no bearing in the hot region of the furnace.

The systems used to simulate the metal and salt phases were (1) water and acetylene tetrabromide in xylene or (2) water and carbon tetrachloride. Water alone was used in many runs for determining pumping rates, mixing power, and residence-time distribution with different mixer designs.

The solvents used in studying extraction efficiency were Mg-42 at. % Cu and $MgCl_2$-30 mol % NaCl-20 mol % KCl-3 mol % MgF_2, selected from the plutonium purification steps of the Salt Transport Process flowsheet.

A. Design of Mixing Chamber

Although a square mixing chamber was incorporated in the design, vortexes formed during operation of the stepped mixer-pump. The first task, therefore, was to eliminate gas entrainment into the mixing chamber by modifying the equipment. In these runs, a plate containing no inlet orifice was installed on the bottom of the mixer-pump to allow mixing to be observed in the absence of pumping. The first modification was the installation of a vertical mixing baffle at each corner of the mixing chamber. These baffles reduced gas entrainment, but entrainment was still excessive. Entrainment was markedly reduced by terminating the vertical baffles at the top of the smaller (4.8-cm ID) portion of the pump and installing a horizontal baffle above the vertical baffles at the bottom of the larger (7.3-cm ID) portion of the pump. Finally, a cylindrical insert was placed in the mixing chamber above the horizontal baffle, and strong vertical recirculation in the upper region (formerly promoted by the drag on the pump wall and the baffling effect of the square mixing chamber) was prevented. This final modification completely eliminated entrainment.

The improvement in entrainment level can be seen by comparing photographs of a mixer-pump operated in water at about 700 rpm with (1) vertical baffles only (Fig. 6), (2) vertical baffles and a horizontal baffle (Fig. 7), and (3) vertical and horizontal baffles and a cylindrical insert (Fig. 8).

Several mixer blade and baffle arrangements were investigated in an effort to promote internal circulation patterns in the mixing chamber that minimize the proportion of liquid having a very short residence time in the mixing region. The mixing intensity for each arrangement was measured

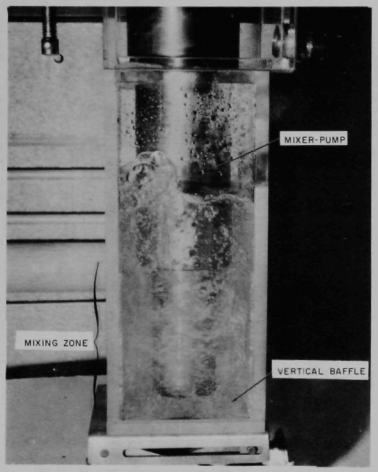

Fig. 6. Air Entrainment in Mixer Stage with Vertical Baffles Only (700 rpm). ANL Neg. No. 308-2344A.

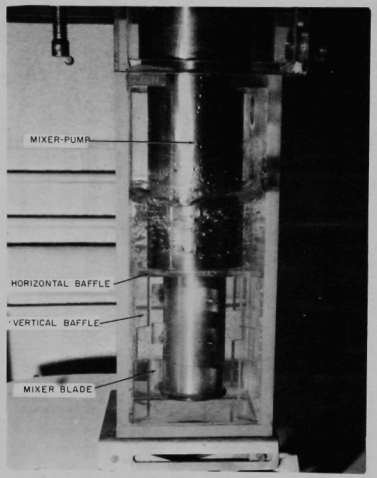

Fig. 7. Reduced Air Entrainment in Mixer Stage with Horizontal Baffle Added (700 rpm). ANL Neg. No. 308-2346A.

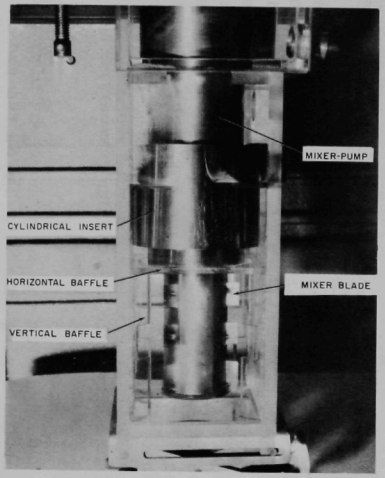

Fig. 8. Air Entrainment Eliminated in Mixer Stage with Cylindrical Insert Added (700 rpm). ANL Neg. No. 308-2345A.

with the aid of a mixing dynamometer.[10]

Ultimately, the configuration represented in Fig. 9 was selected as the final design. The mixing region is divided into two zones in series, connected by a narrow annulus between a horizontal baffle and an opposing horizontal baffle attached to the rotating mixer-pump. A set of six mixing blades is provided in each zone. Figure 9 illustrates the basic features of the mixing chamber, settling chamber, and flow-control weirs. In this design, salt and metal are fed into the mixer at levels above the mixing chamber. The elevation of the salt and metal feed points is determined by the elevation of the settlers and is the same for each mixer; the salt feed point is higher than the metal feed point. The settler that receives fluid from a mixer is physically offset from the mixer to allow flow of either salt or metal (as desired) to the mixing chamber of the adjacent stage without the use of connecting lines.

Both phases flow downward from the zone above the mixing chamber through the two zones of the mixing chamber. Here, the phases are vigorously agitated and eventually enter the bottom of the pump through the inlet orifice. The mixed phases are then pumped up to the collecting chamber and flow into the settling chamber. The inverted cup surrounding the pump outlet eliminates splashing. In the settling chamber, the fluids separate--the light (salt) phase flows out through an overflow spout, and the heavy (metal) phase flows under a baffle and through an overflow spout. The flow is either back to the same mixing chamber or to the mixing chamber of the adjacent stage.

The liquid levels in a settling chamber are fixed by the vertical position of the outlet spouts (see Fig. 9). The volume of each liquid phase in the settling chamber is also fixed. In all stages but stage 5 in Fig. 1, a constant quantity of captive phase is present. Since the quantity in transit in the pump and collecting ring is small and relatively constant, the amount of captive phase in the mixer can be controlled by selecting an appropriate total inventory of that phase in the stage. The flow capacity of the pump and the net flow rate of the other phase establish the salt-to-metal ratio and the total holdup in the mixing chamber. For stage 5, the metal and salt flow rates establish the salt-to-metal ratio.

B. Mixing Power and Pumping Rate

Mixing power results for runs in which water was agitated with no net flow through the pump are presented in Fig. 10. The mixing power induced was found to be very nearly that which would be predicted for two independent six-blade turbines.

Pumping rate data were obtained for all pump configurations studied. Water flow rates are presented as a function of mixer-pump speed in Fig. 11 for a 7.3 cm ID by 4.8 cm ID pump of the final design (Fig. 9) with three different orifice sizes and with the pump discharge port 16 cm above the water level. These results display a characteristic leveling of flow rate at higher mixing speeds. This leveling-out is a result of flow through the orifice being limited by the pressure of the liquid, which in turn is related to the depth of pump submergence in the liquid. This effect allows

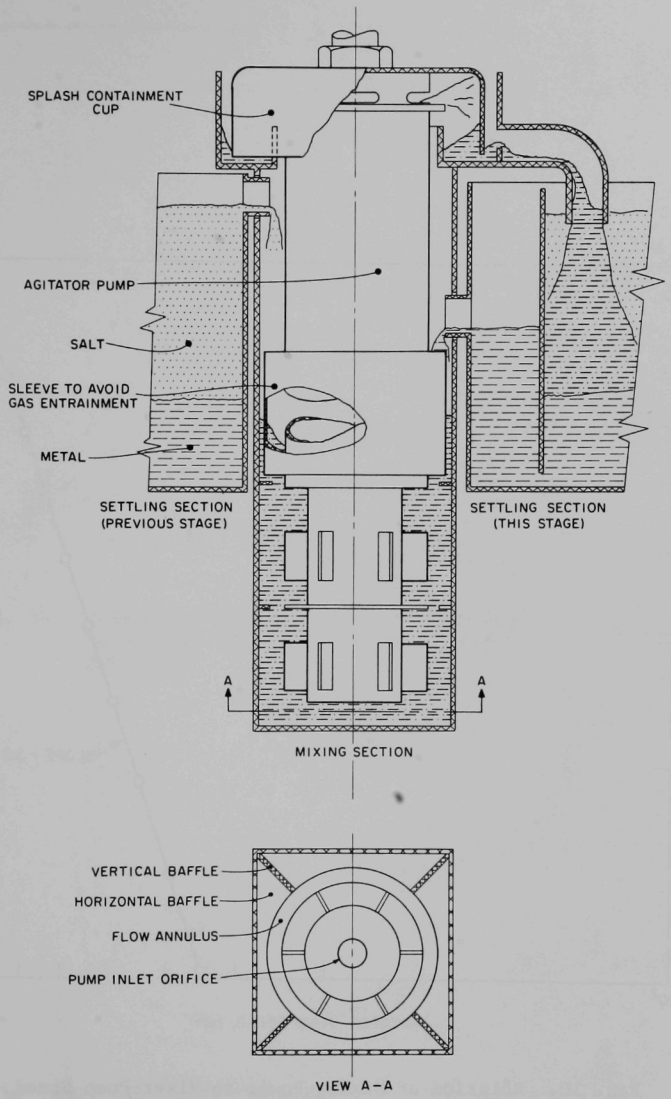

Fig. 9. Typical Mixer-Settler Stage with Captive-Metal Phase. ANL Neg. No. 308-1897.

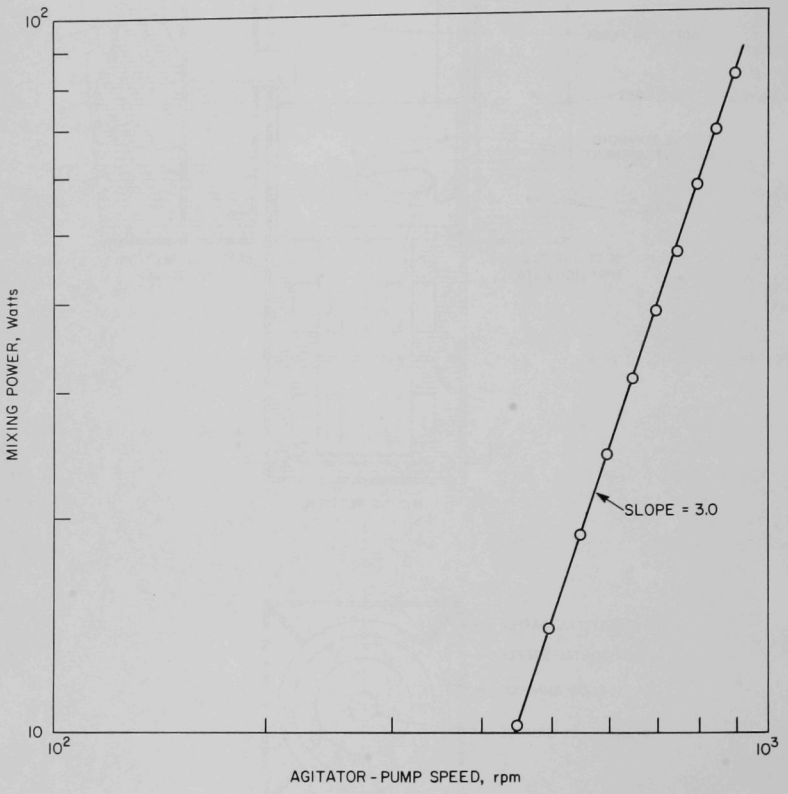

Fig. 10. Relation of Mixing Power to Mixer-Pump Speed. ANL Neg. No. 308-1888 Rev. 1.

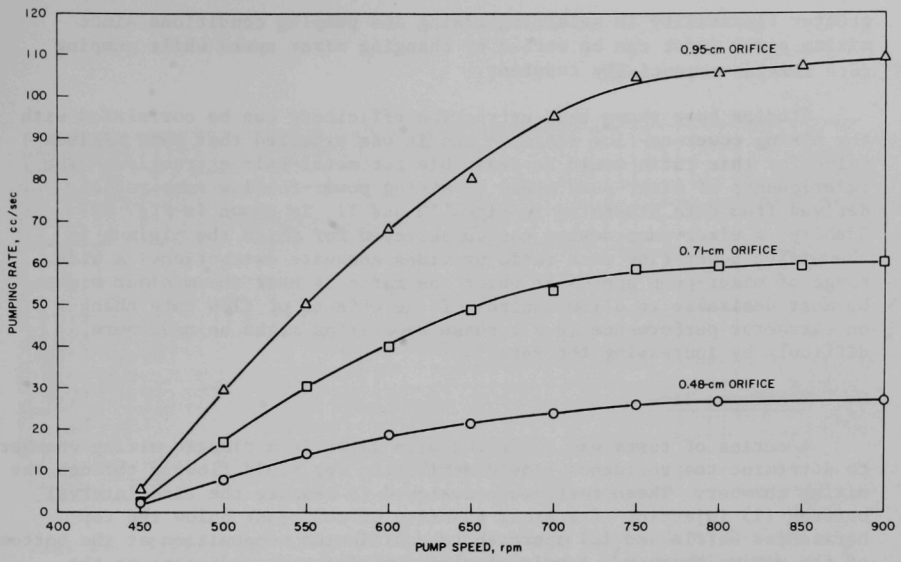

Fig. 11. Effect of Orifice Size and Mixing Speed on Output of Mixer-Pump (Net pumping lift = 16 cm). ANL Neg. No. 308-1890.

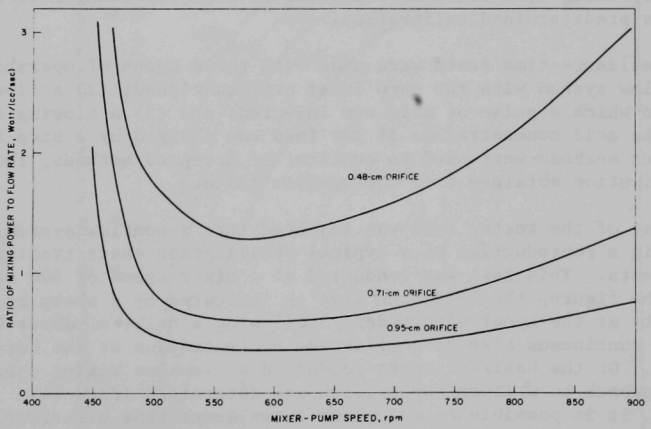

Fig. 12. Effect of Mixer-Pump Speed upon Mixing Intensity (see Fig. 9 for Mixing Chamber Configuration). ANL Neg. No. 308-1887.

greater flexibility in selecting mixing and pumping conditions since mixing power input can be varied by changing mixer speed while pumping rate remains essentially constant.

Studies have shown that extraction efficiency can be correlated with the mixing power-to-flow ratio,[11] and it was expected that some minimum value for this ratio would be desirable for metal-salt extraction. The relationship of mixer-pump speed to mixing power-to-flow rate ratio derived from data presented in Figs. 10 and 11, is shown in Fig. 12. Ideally, a mixer-pump design can be selected for which the minimum in the mixing power-flow rate ratio provides adequate extraction. A wide range of mixer-pump speeds at which the ratio is near the minimum might be most desirable to allow control of the effects of flow rate changes on extractor performance (e.g., phase separation might be made more difficult by increasing the ratio).

C. Residence Time

A series of tests was conducted with water in a plastic mixing chamber to determine the residence time distribution for fluid flowing through the mixing chamber. These tests were designed to measure the time interval between (1) injection of a small quantity of acid just below the top horizontal baffle and (2) approach to equilibrium composition at the bottom of the mixing chamber. A pair of platinum electrodes adjacent to the injection point signaled the start of injection, and a pair of electrodes at the bottom of the mixing chamber (close to the normal pump orifice position) sensed the rise in solution conductivity at that point. A Midwest Model 1210 high-speed recording oscillograph was used to record conductivity changes, which were converted to molarity changes in accordance with a predetermined calibration.

The residence-time tests were made with three modes of operation: (1) a nonflow system with the pump inlet orifice closed; (2) a flowing system into which a pulse of acid was injected; and (3) a flowing system in which the acid concentration of the feed was changed by a step function. The last two methods were used to confirm, by accepted methods, the residence time distribution obtained from the nonflow tests.

In most of the tests, acid was injected into a nonflow system. Figure 13 is a reproduction of a typical oscillograph chart tracing for one of these tests. This test was conducted at a mixer speed of 600 rpm. As shown in the figure, the injection time is indicated by a sharp rise in conductivity at the upper electrodes. Following a delay of about 0.2 sec, there is a continuous rise to equilibrium concentration at the bottom electrodes. On the basis of tests conducted at various mixing speeds, the rate of approach to uniform composition was determined (Fig. 14). From these data, it is possible to calculate a residence time distribution curve for any net flow through the mixing chamber.

Figure 15 shows the rate of approach to uniform composition with three different baffle configurations in the mixing chamber: (1) no center horizontal baffle, (2) with the standard center horizontal baffles (0.6-cm annulus), and (3) with a narrower annulus between the center horizontal baffles (0.3-cm annulus). From these data, effective recirculation

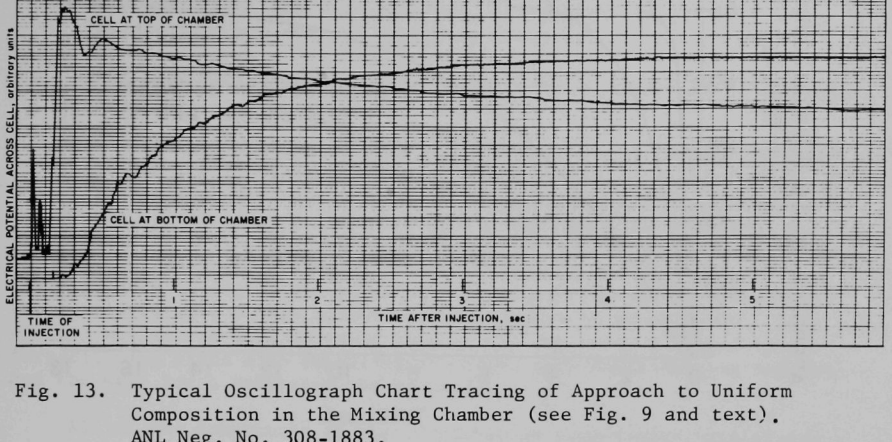

Fig. 13. Typical Oscillograph Chart Tracing of Approach to Uniform Composition in the Mixing Chamber (see Fig. 9 and text). ANL Neg. No. 308-1883.

Fig. 14. Effect of Mixing Speed on Approach to Uniform Composition (see Fig. 9 and text). ANL Neg. No. 308-1881.

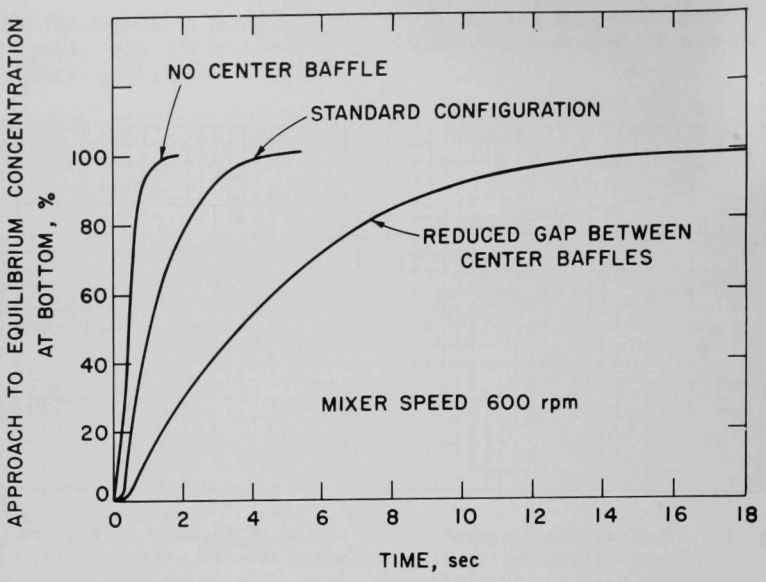

Fig. 15. Effect of Mixing Chamber Baffle Configuration on Rate of Approach to Uniform Composition

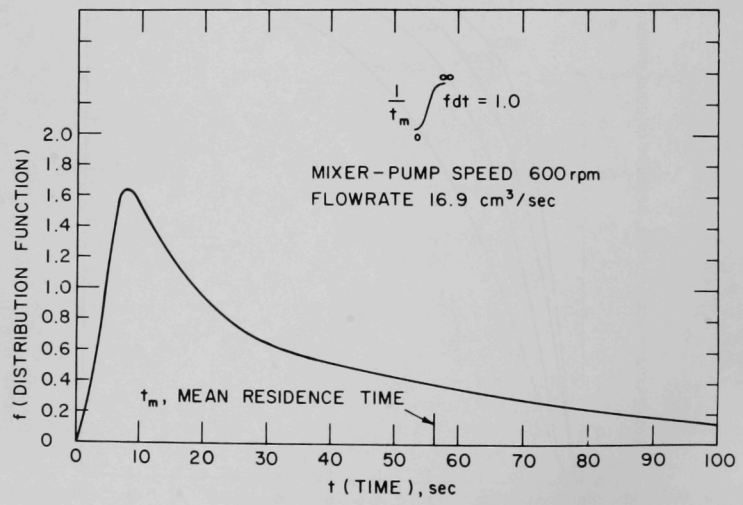

Fig. 16. Residence Time Distribution for Typical Operating Conditions

rates between the upper and lower portions of the mixing region were calculated to be 530, 180, and 50 cm^3/sec for the three baffle configurations.

Figure 16 is a residence time distribution curve for a geometry, flow-rate, and speed typical of that expected for metal-salt extraction. The curve was determined from data obtained with a flowing system in which the acid concentration was changed by a step function.

D. Design and Operation of Mixer-Settler Used to Investigate Extraction Efficiency

The apparatus was designed to fit the cylindrical furnace that had been used for the liquid-metal pumping tests described in Section II of this report. The mixer-settler components included a mixing chamber, a mixer-pump, a settling chamber (which also was the salt reservoir), a metal flow-rate metering cup, a flow diverter for the pump output to bypass the settling chamber, a reservoir tank for metal, and displacement (or "trim") tanks to adjust the level of molten material in the reservoirs. Ports at strategic points allowed liquid samples to be obtained. All control mechanisms were actuated through the top cover plate of the furnace. The plate also supported the mixer-pump shaft bearing and seal and the well for a submerged thermocouple.

All of the components of the single-stage high-temperature mixer-settler were made of Type 304 stainless steel (generally 0.32-cm sheet). They were shaped to fit into a container 31-cm ID by 65-cm tall which, in turn, fit into a gas-tight stainless steel vessel located within a cylindrical resistance-heated furnace. The heating elements of the furnace were divided into vertical zones, permitting some independent control of the temperatures in the top, middle, and bottom zones. Figure 17 is a cutaway sketch of the internal components. Figures 18 through 22 are photographs of these components.

To allow calculation of charge sizes for the extraction runs, the significant areas and volumes of the components were determined by calibration with water. The results are presented in Appendix D. An approximate determination (also in Appendix D) was made of the total dynamic holdup in the pump, collection chamber, settling chamber, and orifice cup when the stage was in operation.

The performance of the liquid level probe was checked with mercury to establish that the output signal was linear with metal level. (It was assumed that the absolute signal output with copper-magnesium alloy would differ from the output obtained with mercury.)

The charging procedure began with introduction of 55.2 kg of crushed ingots of Mg-42 at. % Cu into the sump and melting under argon. The furnace was cooled to 300°C to freeze the alloy, 4.6 kg of extraction salt ($MgCl_2$-30 mol % NaCl-20 mol % KCl-3 mol % MgF_2) was added to the settling chamber, and 0.7 kg of cover salt (KCl-50 mol % LiCl) was added to the metal-alloy sump to minimize magnesium vaporization. The salt was melted. Liquid levels were checked, and metal and salt quantities were adjusted by addition and removal. The total charge of Mg-Cu was about 60 kg

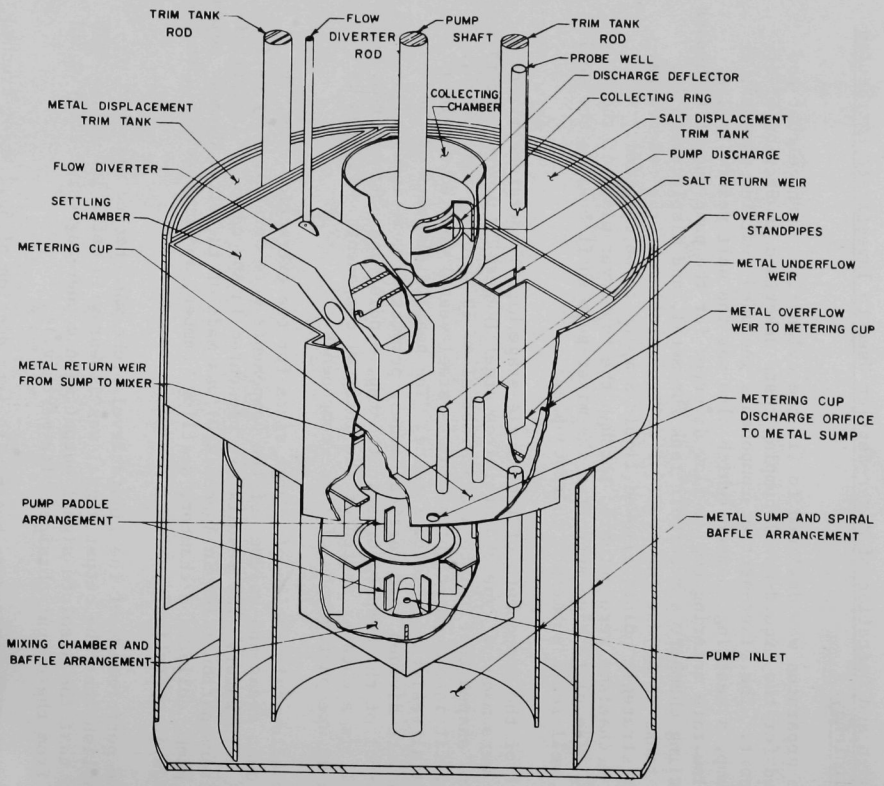

Fig. 17. Internal Components of Single-Stage Mixer-Settler for Molten Salt and Metal Alloy Extraction Studies. ANL Neg. No. 308-2343.

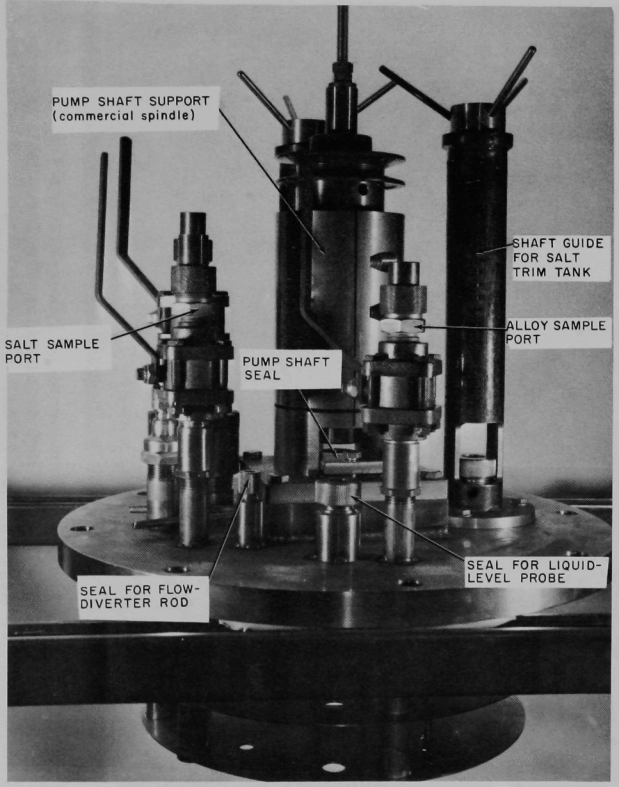

Fig. 18. Cover Plate of Single-Stage Mixer-Settler Furnace. ANL Neg. No. 308-2348A.

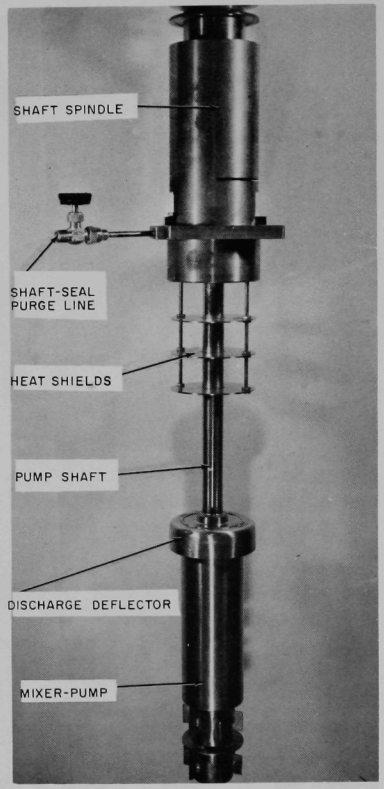

Fig. 19. Mixer Pump and Shaft Assembly. ANL Neg. No. 308-2347A.

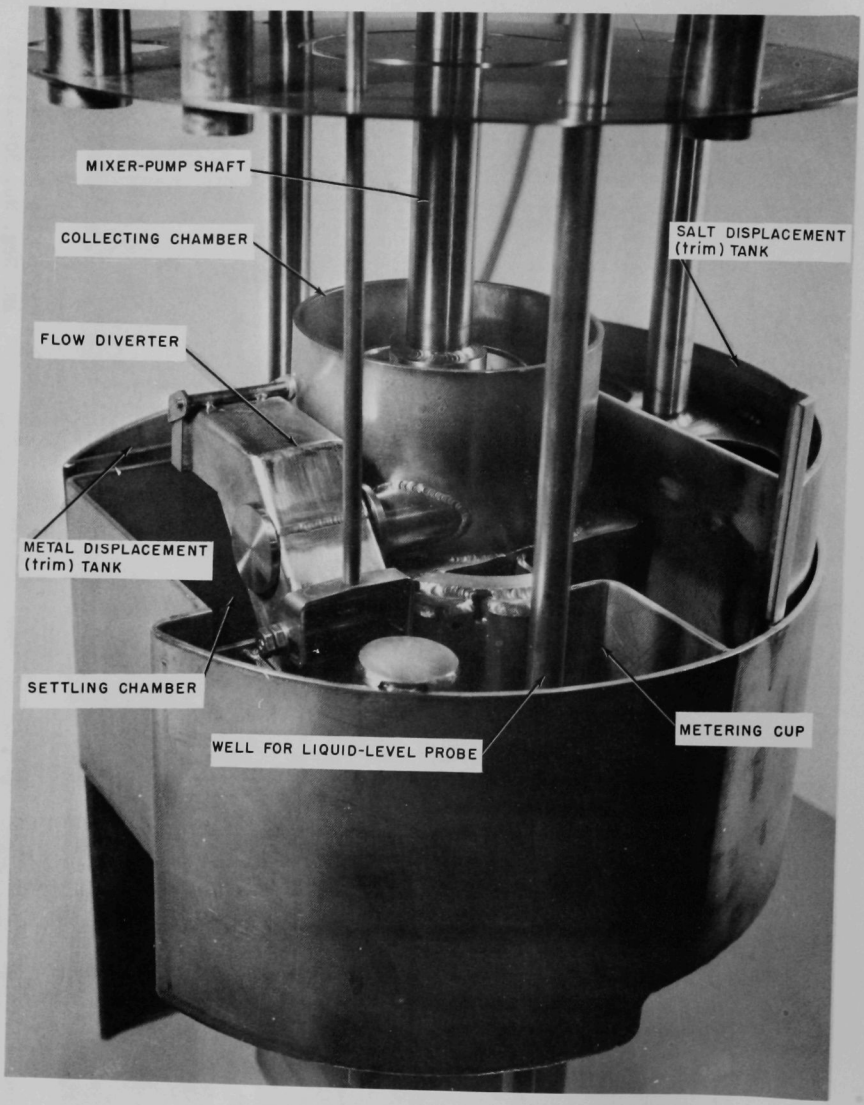

Fig. 20. Assembled Components of Mixer-Settler for Molten Salt and Metal Alloy Studies. ANL Neg. No. 308-2350A.

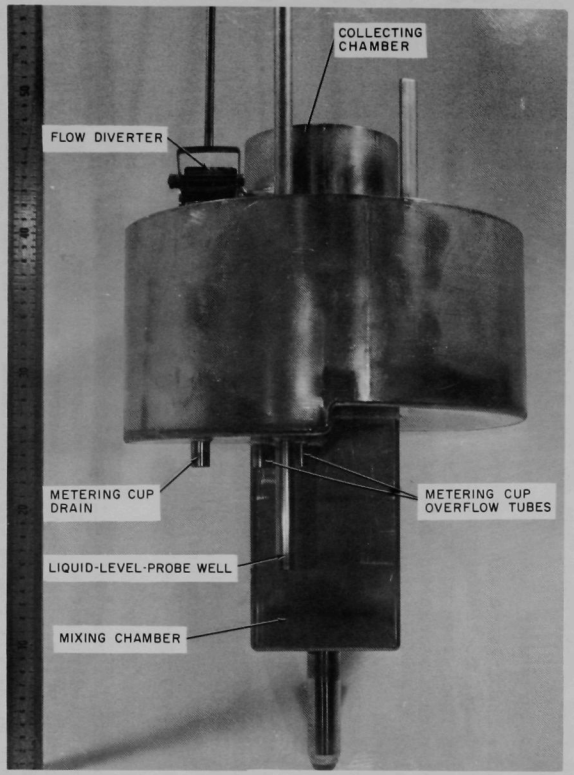

Fig. 21. Side View of Mixer-Settler Assembly. ANL Neg. No. 308-2351A.

Fig. 22. Top View of Metal Sump Showing "Spiral" Path. ANL Neg. No. 308-2349A.

and the charge of $MgCl_2$-$NaCl_2$-KCl-MgF_2 was about 4.0 kg.

The metal-flow-rate metering cup was calibrated by determining drainage curves (as was discussed in Section II). The calibration tests indicated that the original orifice in the cup was too large, resulting in low metal levels in the cup and low readings at the proposed extraction flow rates. The orifice size was reduced from 0.89-cm dia to 0.63-cm dia, and new drainage curves were obtained. An orifice coefficient was calculated from the calibration results, and the surprisingly high value of 0.80 was obtained. (The Reynolds number through the orifice was about 5000, and the expected orifice coefficient was about 0.62.)

The part of the drainage curves representing the time immediately after pump shutdown did not have the expected shape and was not used in the calibration. This effect is attributed to metal contained in the collector ring and the diverter tube continuing to drain into the meter cup after pump shutdown. As a result, initially the molten metal level in the cup did not drop as rapidly as it should. A best-fit curve was made from 13 runs, and this curve was extrapolated to give values for a nearly full metering cup.

Problems were encountered in the operation of the metering cup, apparently because of sludge around the orifice or on the well containing the liquid level probe. The problem was largely eliminated by use of a 0.6 cm dia vibrator rod inserted through a sample port. The rod rested on the bottom of the meter cup and was tapped steadily by an air-driven vibrator.

Since the furnace was operated so that the metal sump was in the coolest region, corrosion products collected there. The corrosion product content of the system was unusually high because of the inadvertent use of a nickel-rich alloy in fabricating a part of the mixer-pump. When the Mg-Cu alloy was first charged, the nickel from the part dissolved completely in the Mg-Cu, and the part quickly corroded away. The pump was removed and the missing part replaced with a stainless steel part, but an excessive amount of finely divided iron and chromium (which have low solubilities in Mg-Cu) remained in the system.

After the metal and salt were charged in the desired quantities, pumping tests were performed. The two general objectives were (1) to verify that pump output during pumping of molten metal was comparable to pump output during pumping of water and (2) to calibrate the pump output (i.e., flow rate) at various pump speeds and various positions of the metal and salt trim tanks.

The initial pump calibration tests with Mg-Cu were made with the same stainless steel pump that had been placed in a plastic mixing chamber and used to pump water. With equal submergence and pump speeds, volumetric flow rates for metal and for water agreed very well. The output of the pump when only metal was pumped was established for various positions of the metal trim tank. Adjusting the metal trim tank downward added metal to the mixing chamber and thus increased the pumping rate at a given pump speed. The position of a trim tank was monitored by measuring the length of threaded drive rod extending above the drive nut.

Since there was no way to measure the salt flow rate directly, this rate was calculated. The salt-to-metal ratio in the mixing chamber was varied from zero to ∿3.5 by appropriately displacing salt and metal with the trim tanks. Salt flow rate was taken as the difference between (1) the metal flow rate through the meter cup at a particular pump speed if only metal were flowing and (2) the observed metal flow rate at that pump speed when both metal and salt were flowing. Because mixing was good, the salt-to-metal ratio in the mixing chamber was equal to the ratio of salt flow rate to metal flow rate. Typical flow data are presented in Fig. 23. A feasible range of total flow rate was ∿22 to ∿55 cm^3/sec. Since the volume of the mixing chamber below the top horizontal baffle was 860 cm^3, these flow rates are equivalent to mean residence times in the mixer of 38 to 16.5 sec.

E. Investigation of Extraction Efficiency

A series of five extraction runs was made in which the transfer of cerium from the metal phase to the salt phase was studied. Cerium was selected as the solute to be partitioned for the following reasons: (1) the ^{141}Ce isotope, which is produced readily by neutron irradiation, provides an excellent tracer for analytical purposes, (2) the use of small amounts of solute in each run is desirable to allow sequential experiments, and (3) cerium distributes strongly to the salt phase so that the approach to equilibrium can be determined by sampling only the metal phase.

Cerium containing ^{141}Ce was extracted from a Mg-42 at. % Cu alloy into $MgCl_2$-30 mol % NaCl-20 mol % KCl-3 mol % MgF_2. These runs were made at ∿670°C and at mixing speeds of 735 and 785 rpm. Salt-to-metal ratios were varied from about 0.57 to 3.1.

The procedure in the first extraction run for preparing metal alloy containing cerium was as follows: The salt trim tank was raised so that no salt could overflow from the settling chamber, and the pump was operated until all of the salt in the system was contained within the settling chamber. The metal trim tank was then lowered to fill the mixing chamber with metal. The flow diverter was set so that metal flow from the collection chamber was diverted into the metal cup, rather than the settling chamber. The mixer-pump was then operated at a fairly high speed (∿800 rpm) to provide a high rate of metal flow (>50 ml/sec). At this flow rate, the level of metal in the meter cup was high enough so that metal flowed through the two overflow tubes as well as the metering orifice. These streams flowed into the spiral path built into the sump for the metal alloy (Fig. 22).

A charge of Mg-Cu-Ce alloy (containing ^{141}Ce tracer) in a copper tube sealed with magnesium plugs was added to the meter cup through a sample port valve. As the tube dissolved, the cerium alloy dissolved in the Mg-Cu alloy and flowed from the meter cup into the sump. The metal alloy was circulated through the mixing chamber, metering cup, and metal sump overnight (∿14 hr) to assure homogeneoous distribution of the cerium in the alloy. Before an extraction run was made, a set of metal samples were taken at the metal weir sample point to determine the homogeneity of the cerium in the alloy.

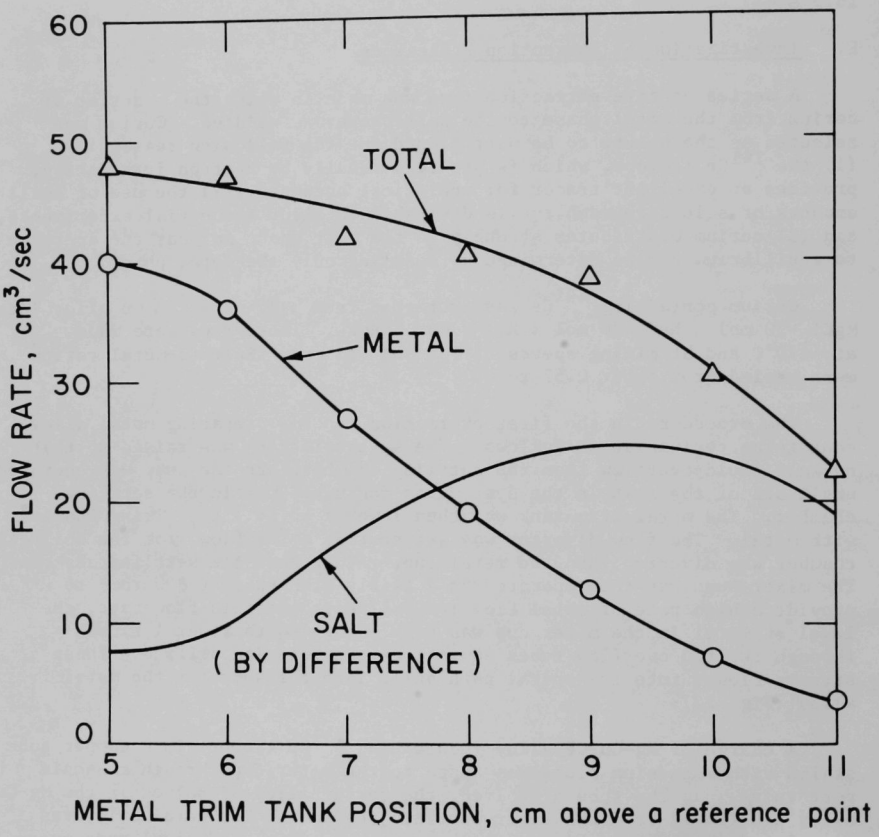

Fig. 23. Effect of Metal Alloy Trim Tank Position upon Metal and Salt Flow Rates (760 rpm)

Since at this time the mixing chamber contained no salt to extract cerium from the Mg-Cu-Ce alloy, precautions had to be taken to avoid introducing an excessive amount of cerium in the alloy entering a run. The bulk of the cerium was removed from the metal in the mixing chamber by a "batch" extraction: The salt trim tank was lowered to add the desired amount of salt to the metal in the mixing chamber, then the mixer-pump was operated for ∿5 min at a low speed (∿400 rpm) so that none of the salt or metal was pumped out. Thereby, the salt and metal were mixed adequately to transfer the cerium to the salt without pumping any of the salt and metal into the settling chamber.

Subsequently, the metal and salt trim tanks were adjusted to give the desired salt-to-metal ratio, the mixer-pump speed was increased to provide the desired flow rate, and the pump discharge stream was diverted so that it flowed into the settling chamber. At operating flow rates, the entire metal stream flowed through the settler, into the meter cup, through the meter cup orifice, and into the sump at the point farthest from the metal inlet to the mixing chamber. The sump functioned as a combined metal feed tank and receiving tank. The spiral path in the sump for the metal flowing out of the meter-cup orifice was designed to minimize bypassing of the depleted metal into the mixing chamber before most of the initial supply of metal in the sump had entered the mixing chamber. A run was continued long enough to ensure that two complete changes of the metal in the sump had been effected.

During a run, samples of the metal leaving the settling chamber were taken periodically and analyzed for ^{141}Ce. A salt sample taken at the completion of the run also was analyzed for cerium. The salt and metal streams were then circulated overnight in an attempt to equilibrate all of the salt with all of the alloy in the furnace. Samples of both phases were then taken to provide equilibrium data.

In extraction run 1, the metal alloy flow rate was 17.5 ml/sec. A salt flow rate of 22.8 ml/sec was planned that would give a salt-to-metal ratio of 1.3. Because of improper adjustment of the salt trim tank, the actual salt rate is estimated to have been about 10 ml/sec and the salt-to-metal ratio about 0.57.

Four samples of the Mg-Cu feed alloy for run 1 showed ^{141}Ce concentrations ranging from 1.23×10^6 counts/(min)(g) to 2.02×10^6 counts/(min)(g) with an average of 1.6×10^6 counts/(min)(g). Samples of the alloy stream flowing out of the settler were taken at 2-min intervals during the extraction period of the run. The ^{141}Ce concentrations ranged from 4.78×10^4 counts/(min)(g) to 5.89×10^3 counts/(min)(g). The average concentration was $\sim 1.5 \times 10^4$ counts/(min)(g). These values indicate that approximately 99.7% of the cerium had transferred from the metal alloy to the salt. Since equilibrium conditions would require a small concentration of ^{141}Ce to remain in the metal alloy, the extraction appears to have reached at least 99.7% of equilibrium. Figure 24 shows the counting rates for ^{141}Ce radioactivity in the metal alloy feed and effluent samples. Sampling of salt and metal at the end of a run did not prove satisfactory for establishing an overall material balance between the cerium removed from the metal alloy and the cerium found in the salt. Concentrations of cerium in the salt samples were low; this probably was because the salt

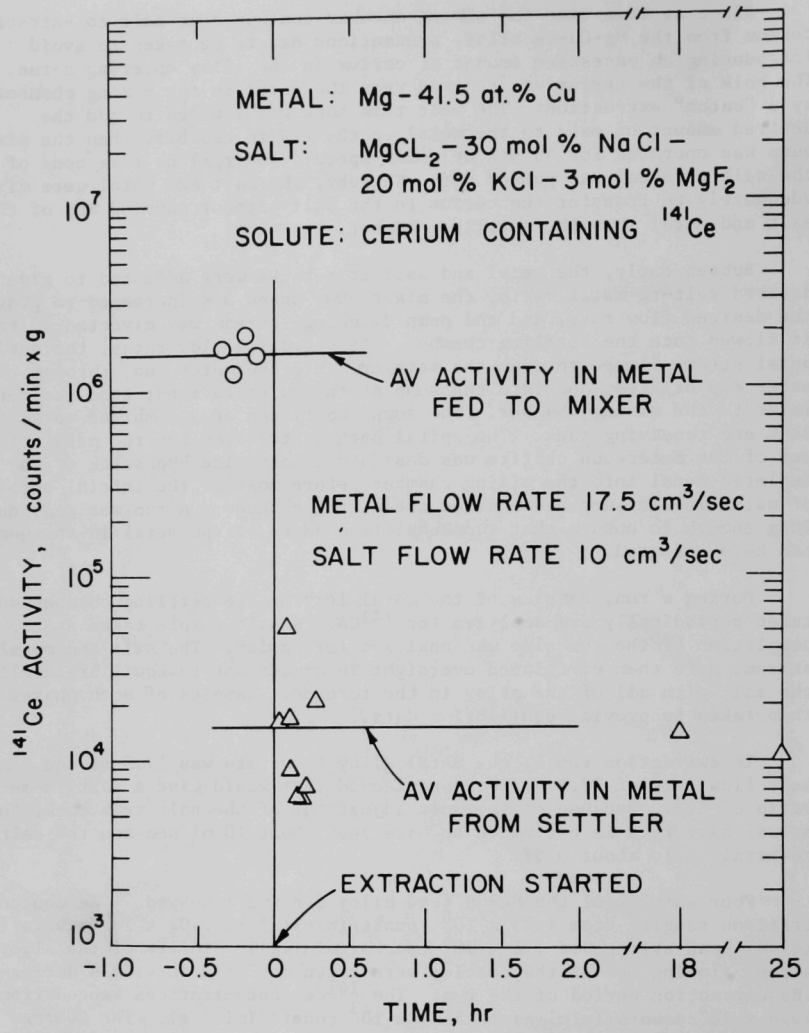

Fig. 24. ^{141}Ce Activity in Metal Alloy Samples from Extraction Run 1 (670°C)

was sampled in a corner of the settling chamber at a point removed from the normal flow path of the salt stream.

Subsequent extraction runs were made by adding additional charges of cerium alloy in the manner described above. The overall effect was a gradual increase in the cerium concentrations in both the salt and metal phases, but these increases did not hinder analytical results since cerium distributed strongly to the salt.

After the addition of a second charge of tagged cerium, run 2 was made under conditions which duplicated the planned conditions of run 1. The metal alloy flow rate was 17.5 ml/sec and the salt flow rate was 22.8 ml/sec to give a salt-to-metal ratio of 1.3. The ^{141}Ce concentration in the feed metal averaged 8×10^5 counts/(min)(g), which was about one-half the concentration used in run 1. The lower ^{141}Ce concentration was a result of both radioactive decay of the ^{141}Ce in the charge alloy and a smaller ^{141}Ce charge to run 2. The concentration of ^{141}Ce in the alloy effluent from the settling chamber ranged from 5×10^3 to 8.5×10^3 counts/(min)(g) and averaged about 7×10^3 counts/(min)(g). These results show that slightly more than 99% of the cerium transferred from the metal alloy to the salt and therefore that the stage efficiency achieved was greater than 99%.

It was subsequently discovered that the metal alloy samples taken in this run, as well as samples taken in run 1, were slightly contaminated with extraction salt. It was not resolved whether the salt contamination had been caused by incomplete phase separation in the settling chamber or by partial plugging of the effluent line from the collecting chamber (see Section F below). The latter could cause some salt and metal to overflow the collecting chamber wall, bypass the settling chamber, and fall into the weir where the metal alloy samples were taken. The salt contamination constituted about 1% of the total metal alloy sample. Because the ^{141}Ce concentration in the salt was about 100 times as high as the activity in the metal, the total ^{141}Ce count found in the sample was essentially equal to the ^{141}Ce activity that could be attributed to the salt. Thus, on a salt-free basis, the ^{141}Ce activity in the metal alloy would be substantially less than that reported above and extraction efficiency in these runs may have been greater than the 99.7 and 99% reported.

Runs 3 and 4 were made at a metal flow rate of 6.3 ml/sec and a salt flow rate of 19.4 ml/sec. The low metal flow rate was selected for runs 3 and 4 in an attempt to increase the settling time and obtain a salt-free effluent. Run 5 was made at a metal flow rate of 24 ml/sec and a salt flow rate of 16.8 ml/sec. The results of these three runs showed that approximately 95% of the cerium had transferred from the metal to the salt. However, in these runs as in runs 1 and 2, the metal alloy samples were contaminated with extraction salt. This suggests that salt spray from the collecting chamber, rather than incomplete settling, caused contamination of the metal alloy samples. Again, the amount of cerium that could be attributed to salt contamination was essentially equal to the total cerium found in the sample. It is therefore reasonable to conclude that the efficiency of extraction of cerium from the metal alloy into the salt was greater than 99%.

F. Equipment Performance

The overall mechanical performance of the single-stage mixer-settler is considered satisfactory. Some components operated with very high reliability, while others showed deficiencies that adversely affected the performance of the entire system.

Mechanical performance of the mixer-pump and bearing assembly was very good. Total running time of the pump was approximately 1300 hr at temperatures above 650°C. There was no evidence of shaft deflection or dynamic imbalance. This performance confirms the reliability of the design in which the shaft bearings were located above the furnace cover and completely out of the heated zone. The commercial spindle used as the shaft bearing gave excellent service.

The shaft seal was adequate for its application. The seal was a simple compression seal using packing rings made of braided asbestos impregnated with molybdenum disulfide. A lantern ring distributor located below the packing housing provided an argon purge at slightly elevated pressures to prevent penetration of fumes from the furnace into the seal. The seal had been designed for use on a multistage extractor that was intended for operation in an inert atmosphere. Consequently, it was not designed to be vacuum-tight since contamination by air leaking into the equipment would not occur. In an air atmosphere, the seal was not tight enough to permit complete evacuation of air from the furnace after it had been opened and resealed. This condition resulted in slight oxidation of magnesium fumes.

Many of the operating problems resulted from suspended corrosion products. A major source of these corrosion products probably was inadvertent incorporation of an Inconel part into a pump that was used during the initial testing of the equipment. The Inconel part corroded away completely.

The Type 304 stainless steel used for fabricating the components was not completely resistant to the Mg-Cu alloy, but there was no evidence of severe corrosive attack except on the mixer blades and baffles. The blades were originally 0.050 in. thick. Following the tests, the upper blades were about 0.044 in. thick and the lower blades were about 0.028 in. thick. All blades were corroded most severely near the tips. The decrease in thickness of the horizontal baffle on the pump was from 0.050 to 0.035 in.

Corrosive attack was by leaching of nickel from the stainless steel; the quantities of iron and chromium released exceeded their solubilities in the alloy, and a sludge formed. During one overnight period, the temperature rose to 800°C for about 3 hr as a result of a faulty heater relay. The system was then returned to the operating temperature of ~670°C. The high temperature probably led to a significant increase in nickel leaching and an increased quantity of sludge. Sludge accumulated at constrictions in the metal flow path such as the underflow weir in the settling chamber, the orifice in the meter cup, the collector ring at the mixer-pump discharge, and the flow diverter.

When the furnace was opened for inspection at the conclusion of the series of extraction runs, a large accumulation of metal alloy was found on the inside wall of the furnace at the level of the collecting ring. The appearance of this material indicated that it had been slung out of the collecting chamber by the discharge deflector (see Fig. 17). This condition could occur only if the deflector were rotating within a relatively deep pool of molten alloy and salt. Such an accumulation would be the result of a restriction to flow in the flow diverter caused by an accumulation of sludge within the diverter. Presumably, it was under these circumstances that the contamination of metal samples by extraction salt (described in Section E above) occurred.

While this deficiency in the operation of this single-stage mixer-settler was unfortunate, a similar deficiency would not be expected in a multistage unit. The use of the flow diverter in the single-stage unit led to the flow restriction. In a multistage mixer-settler, the metal alloy and salt would flow directly from the collecting chamber into the settling chamber. Furthermore, a multistage unit would be made of (or protected by) refractory metals which would be more resistant to attack by the process materials.

IV. CONCLUSIONS

The operation of the single-stage mixer-settler has demonstrated that the basic design of a multistage high-temperature mixer-settler is sound. The limited number of tests performed to measure stage efficiency has demonstrated that very high stage efficiencies are achieved as a result of effective phase contacting within the mixing chamber. The mixer-pump functioned in a highly satisfactory manner, with respect to both mixing and pumping of the molten metal and salt.

The metal and salt trim tanks were effective means of regulating the quantity of salt and metal in the flowing system. The same technique is expected to be suitable for a multistage extraction bank.

The principal difficulties encountered in the operation of the single-stage furnace resulted from suspended corrosion products in the metal alloy. For long-term operation of a multistage system, either fabrication of the components of a refractory material such as molybdenum-tungsten alloy or protection of stainless steel components by a refractory covering would be highly desirable.

The metering cup combined with the induction probe was an effective means of measuring flow rate of the metal alloy. However, the presence of sludge in the metal alloy reduced the effectiveness of the measuring technique. In a clean molten metal system, the metering cup and induction probe are expected to function accurately and reproducibly.

The design of a seven-stage mixer-settler was carried to the extent of layout of individual stages, interstage flow passages, interstage pumps, metering cup, transfer lines, the mixer-pump drive assembly, the furnace enclosure, and heaters. Because of budgetary limitations, the program for the Salt Transport Process was terminated before detailed designs could be

completed. The same budgetary limitations precluded any effort to modify the single-stage mixer-settler and make additional runs to establish that adequate phase separation could be achieved.

APPENDIX A

SALT TRANSPORT PROCESS FOR LMFBR FUEL

The Salt Transport Process is intended to provide a plutonium recovery of at least 99% from stainless steel-clad uranium-plutonium oxide LMFBR fuels. As is indicated in Fig. 25, decladding is accomplished by immersing fuel subassemblies in liquid zinc at about 850°C. (A cover layer of $CaCl_2$-CaF_2 inhibits zinc vaporization.) The stainless steel dissolves in the zinc, and this solution is transferred out of the decladding vessel; the unaffected fuel oxide remains in the vessel. It is anticipated that during this operation some gaseous fission products will be released from the fuel.

Oxide reduction is performed in the same vessel as decladding. The uranium oxide and plutonium oxide constituents of the fuel are converted to metal by vigorous contacting at 800°C with a liquid Mg-29 at. % Cu-34 at. % Ca alloy in the presence of molten $CaCl_2$-20 mol % CaF_2 salt. The alkali, alkaline earth, and iodine fission products are taken up by the salt; also, it is expected that during this reduction reaction, the remainder of the gaseous fission products will be released from the fuel. When reduction is complete, the metallic plutonium is in solution in the liquid metal phase, and the uranium is in the form of a bed of precipitated metal.

Plutonium purification (described in detail in Appendix C) starts with the extraction of rare earth fission products and fission product yttrium into a salt stream (later discarded as waste) in the first four stages of a seven-stage mixer-settler. In the next two stages of the mixer-settler, the plutonium is separated from the nobler fission product elements by extracting the plutonium into a salt stream while the nobler fission products remain in the Cu-Mg alloy. In the last stage of the mixer-settler, the purified plutonium is extracted into Zn-Mg alloy.

The Zn-Mg-Pu alloy may be transferred to a retorting vessel for removal of the zinc and magnesium by vacuum distillation. The plutonium metal product may then be alloyed with metallic uranium in the appropriate proportion and charged to a fluidized-bed reactor where the alloy may be hydrided and dehydrided to form a fluidizable powder that can be converted to UO_2-PuO_2.

Purification of the precipitated uranium metal that remains in the decladding-reduction vessel after removal of the Mg-Cu-Pu solution is also provided by the Salt Transport Process. Uranium dissolved in Cu-14 at. % Mg alloy is fed to a four-stage salt-metal extraction step. In the first stage, any plutonium in the alloy is extracted by contacting the alloy with a salt phase. In the other three stages, the uranium is separated from fission products by extraction into a salt phase, contacting with zinc or cadmium, then extraction into a Mg-Zn alloy, where it accumulates as a precipitate.

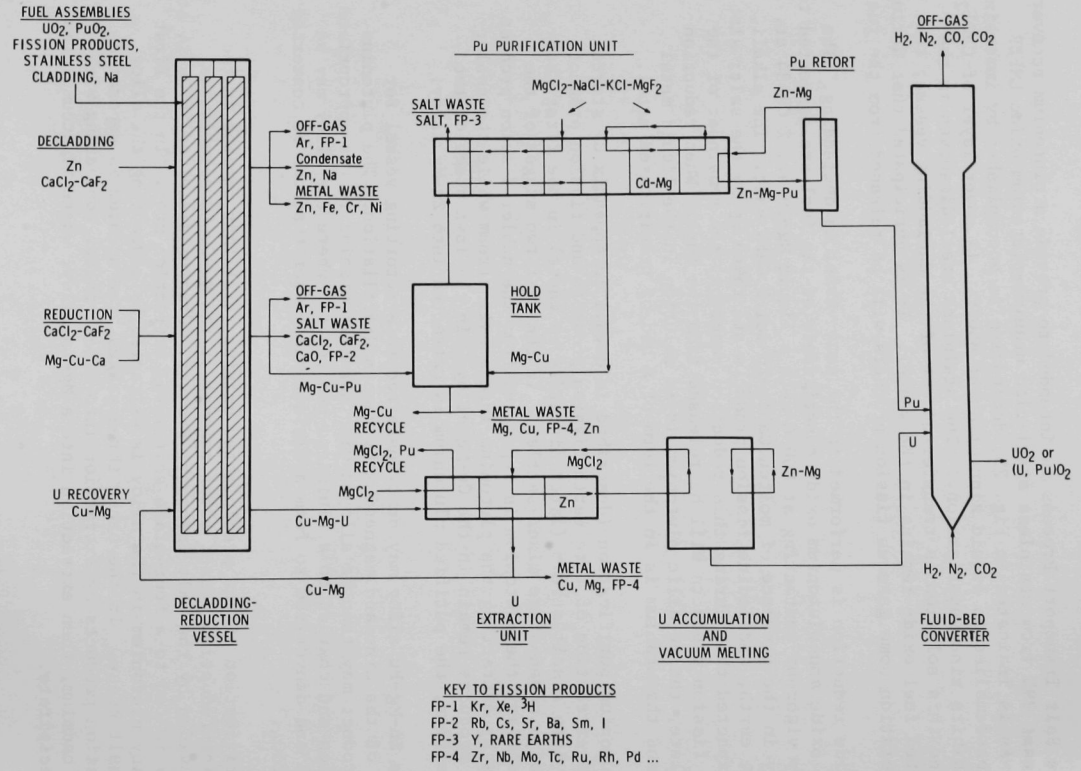

Fig. 25. Salt Transport Process for LMFBR Fuel.
ANL Neg. No. 308-1868 Rev. 1.

APPENDIX B

CHEMICAL BASIS OF SALT TRANSPORT SEPARATIONS

Since purification is effected in a salt transport process by circulating a molten salt between a liquid donor alloy and a liquid acceptor alloy, the degree of separation of plutonium and uranium from each other and from the more noble impurity elements depends primarily upon differences in the distribution of uranium, plutonium, and impurity elements between the liquid metal and salt solvents. As an example, an element, A, partitions between a liquid magnesium alloy and a molten salt phase containing $MgCl_2$ by the following reaction:

$$A(\text{alloy}) + \frac{n}{2} MgCl_2(\text{salt}) \rightleftarrows ACl_n(\text{salt}) + \frac{n}{2} Mg(\text{alloy}), \qquad (1)$$

where A is an element under consideration, and n is the valence of A.

The extractions that can be effected are evaluated from the distribution coefficients attainable. The distribution coefficient, D, for an element A is defined as

$$D_A = \frac{y_A}{x_A} \qquad (2)$$

where y_A is the concentration (mol %) of the chloride of A in the salt,
x_A is the concentration (at. %) of A in the alloy in equilibrium with y_A.

The extraction factor, R, is useful in process design. It is defined as the ratio of the amount of an element in the salt to the amount in the metal:

$$R_A = \frac{S\, y_A}{M\, x_A} = \frac{D_A S}{M}, \qquad (3)$$

where S is the total quantity of salt (moles) and
M is the total quantity of metal (moles).

The separation factor, α, for two elements is defined as the ratio of their distribution coefficients:

$$\alpha_{AB} = \frac{D_A}{D_B} \qquad (4)$$

where A and B are two different elements.

The magnitude of the distribution coefficients is dependent on the equilibrium constant for the reaction (equation 1), the activity coefficients for the components in the metal and salt phases, and the magnesium and magnesium chloride contents of the metal and salt phases. The application and control of these variables in designing chemical separations has been reported.[12] The metal and salt compositions for the present separation operations were selected to optimize plutonium-rare earth separation by

providing distribution coefficients that give desirable extraction factors at convenient salt-to-metal weight ratios.

APPENDIX C

PROCESS STEPS FOR PLUTONIUM PURIFICATION IN A CONCEPTUAL SEVEN-STAGE MIXER-SETTLER

A conceptual seven-stage mixer-settler to separate fission products from plutonium and produce a purified plutonium-zinc-magnesium product is shown schematically in Fig. 26. This concept involves an extraction strategy proposed by W. J. Walsh.[13] The compositions of the process solvents are listed in Table 1.

The first four stages (metal transport) are designed to remove rare earths from the feed solution in a waste salt phase without undue loss of plutonium, using a semicontinuous mode of operation. In the final three stages (salt transport), the nobler metals are separated from plutonium. Extraction is performed as follows:

(1) The donor alloy containing plutonium and fission products is contacted in stages one to four with metal transport salt that extracts the rare earths and some plutonium. The salt is not circulated between stages but is "captive" in each stage. (2) In stage five, plutonium is extracted from the Cu-Mg alloy into a second salt stream (salt transport salt). In this stage, the plutonium extraction factor is increased by increasing the salt-to-metal ratio. (3) The alloy, which now has a low plutonium content, is recycled through the captive salt in stages one to five, and plutonium is stripped from the salt in the early stages and extracted into the salt in stage five. (4) When the level of plutonium in the stage one salt is sufficiently low to allow disposal of this salt without significant loss of plutonium, metal circulation is terminated. (5) The Cu-Mg alloy is removed from the hold tank and recycled to the reduction step. The levels of uranium and nobler metals in the recycled Mg-Cu alloy are controlled by removal of these constituents in the reduction step (Fig. 25) and by discarding a small portion of the Mg-Cu alloy before recycle to the oxide reduction step. (6) Fresh Mg-Cu-Pu-RE-NM-U feed is charged to the hold tank. (7) The salt in stage one, containing most of the rare earths, is discarded. (8) The salt phases in stages two, three, and four are transferred to stages one, two and three, respectively. (9) Fresh salt is added to stage four. (10) Processing of a new batch begins with circulation of the feed alloy (Mg-Cu-Pu-RE-NM-U) through stages one to five.

Selective extraction of plutonium from the nobler elements in stages five to seven is effected[12] as follows: (1) Plutonium is extracted into the salt transport salt stream in stage 5, and the bulk of the nobler metal fission products are retained in the Cu-Mg alloy. (2) The salt is scrubbed in stage six with a captive Mg-Cd alloy for further removal of nobler metals and removal of any feed solvent (Cu-Mg) entrained in the salt stream. The capacity of the Mg-Cd scrub alloy is sufficient for many runs, but eventually the scrub alloy is discarded and replaced. (3) In stage seven, the salt is contacted with a captive Zn-Mg alloy (acceptor alloy) which extracts the plutonium. The salt, which has served only as a transport medium, is recycled to stage five. In normal operation, nothing accumulates in the transport salt, and it can be used indefinitely.

TABLE 1. Plutonium Purification Process Solvents

	Composition	Density at 650°C (g/cc)
Metal Transport - Donor Alloy	Mg-44 at. % Cu	4.0
Scrub Alloy	Mg-20 at. % Cd	2.8
Acceptor Alloy	Zn-30 at. % Mg	5.0
Rare Earth Extraction and Salt-Transport Salts	$MgCl_2$-30 mol % NaCl-20 mol % KCl-3 mol % MgF_2	1.7

TABLE 2. Distribution Coefficients[a]

Salt Solvent: $MgCl_2$-30 mol % NaCl-20 mol % KCl-3 mol % MgF_2
Temperature: 650°C

	D_{Pu}	D_U	D_{Ce}	D_{Zr}
Metal Transport and Donor Alloy (Mg-Cu)	1	0.1	1×10^{3}	6×10^{-3}
Scrub Alloy (Mg-Cd)	0.5	5×10^{-2}	60	2×10^{-3}
Acceptor Alloy (Zn-Mg)	1×10^{-3}	5×10^{-4}	0.2	1×10^{-9}

[a]Distribution coefficient, $D = \frac{\text{mole fraction in salt}}{\text{atom fraction in metal}}$

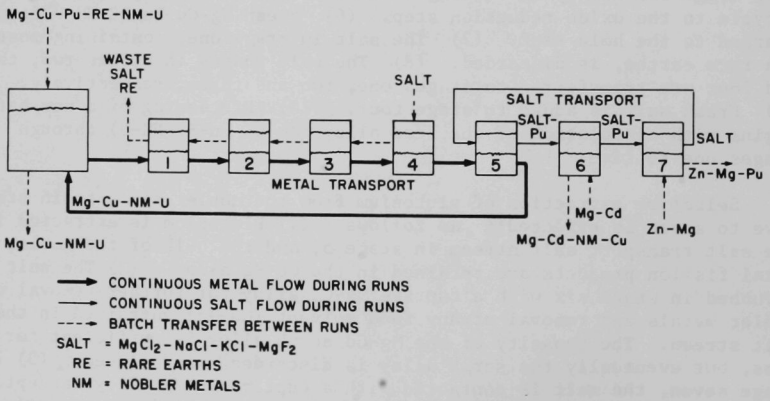

Fig. 26. Plutonium Purification Step of the Salt Transport Process. ANL Neg. No. 308-1879 Rev. 1.

(4) At the conclusion of an extraction run, the acceptor alloy containing the purified plutonium is removed and fresh acceptor alloy is charged to stage seven.

As is indicated in Appendix B, the salt-metal system for the plutonium purification was selected to give adequate separation of plutonium from fission products. Some pertinent distribution coefficients are listed in Table 2. The distribution coefficients are relatively constant over the expected range of solute concentration.

From these distribution data, an excellent separation factor of 1000 is predicted for plutonium and cerium in Mg-Cu solvent. In the salt-donor alloy system, the distribution coefficient for plutonium is unity, allowing extraction of plutonium in either direction by adjustment of the salt-to-metal ratio (Eq. 3, Appendix B). Distribution coefficients in the scrub alloy include desirably low values for nobler metals (zirconium is the nobler metal fission product most difficult to separate) and a sufficiently high value for plutonium to minimize plutonium holdup in the scrub stage. For the Zn-Mg acceptor alloy, the distribution coefficient for plutonium is low, as is necessary to extract plutonium out of the transport salt. It is concluded that the conceptual seven-stage mixer-settler should provide the desired decontamination factor of 10^6. However, one or two additional stages can be added if extraction experience indicates they are necessary.

APPENDIX D

CALIBRATION OF SINGLE-STAGE MIXER-SETTLER

The various chambers of the apparatus were calibrated. Water was used in determining their areas and volumes and the elevations of spillover weirs.

The following dimensions were determined for the key zones of the unit:

Area of settling chamber	353 cm^2
Area of metal sump	684.6 cm^2
Area of salt trim tank	146 cm^2
Area of metal trim tank	90.6 cm^2
Area of mixing chamber	94.3 cm^2
Area of meter cup	97.1 cm^2
Height of salt overflow weir above bottom of settling chamber	10.1 cm
Height of metal overflow weir above bottom of settling chamber	6.1 cm
Total volume of settling chamber (with salt trim tank removed)	3560 ml
Total volume of metal sump (with metal trim tank removed)	14.53 l
Volume of mixing chamber to top horizontal baffle, with mixer-pump in operation (i.e., "effective operating volume")	860 ml
Height of overflow standpipes in meter cup above orifice level	5.67 cm

From the relative areas of trim tanks and chambers, the effect of vertical movement of a trim tank upon the level of the molten material in which it is immersed can be calculated. Thus, in the settling chamber, the net area outside of the trim tank is 207 cm^2. Consequently, a vertical displacement of 1 cm by the trim tank results in an increase or decrease in salt level of 146/207 = 0.705 cm.

Similarly, a vertical displacement of 1 cm in the metal trim tank results in an increase or decrease in metal level of 90.6/594 = 0.152 cm. The salt trim tank was made large with respect to the salt volume in the settling chamber, since it is necessary to use the trim tank displacement to provide a space in which to transfer all of the salt from the mixing chamber into the settling chamber.

The ratio of the area of the salt trim tank to the area of the metal trim tank is 146/90.6 or 1.6. Accordingly, when one phase is to be replaced

by the other in the mixing chamber, a change in elevation of 1 cm in the salt trim tank is equivalent to a change in elevation of 1.6 cm in the metal trim tank.

Not only were the area and volume of the settling chamber calibrated under static conditions but also the increased phase holdup under dynamic conditions was measured approximately. This added holdup allows for the hydraulic head needed to produce the required flow through the chamber and over the weirs, as well as accumulations within the collection chamber and metering cup. This additional dynamic inventory was estimated to be 378 ml, based on measurement with water flowing at about 40 ml/sec.

The holdup of metal alloy and salt in the settling chamber could be determined only by a calibration with the process salt and alloy at operating temperature. The metal level is set at the level of its overflow weir by running the pump at a low rate and noting the flow into the meter cup by use of the level probe. The elevation of the top of the salt in the settler is determined by the action of the salt trim tank. With the mixer pump off, the trim tank elevated, and all the salt in the settler, the trim tank is slowly lowered until the liquid level probe shows a very small rise indicating that some metal has flowed over the metal weir. This indicates that the bottom of the salt trim tank has made contact with the molten salt surface and the increased salt level has forced some metal over the weir. Based upon the dimensions of the salt trim tank and the settler, the depth and volume of salt can be calculated.

Based on pumping rate calibrations with water, a pump inlet orifice of 0.72 dia was selected to obtain a total pumping rate ranging from 54 to 60 ml/sec at speeds of 700 to 900 rpm. This orifice size proved satisfactory with the metal-salt system.

The meter cup orifice was initiatially 0.89 cm dia. This size was selected to provide adequate levels of metal in the meter cup for measurements of normal metal flow rates, yet allow for overflow through the meter cup standpipes at maximum pump output rate. Later, the orifice diameter was reduced to 0.63 cm when experience showed the operating level in the meter cup was less than expected.

ACKNOWLEDGMENTS

The authors wish to acknowledge the contributions of D. S. Webster for his overall guidance of the program, of W. E. Miller for initial studies of mixer pumps, of W. J. Voss for fabrication of plastic models of test components, of A. E. Lissy for radiological monitoring during extraction runs, of Z. Tomczuk and C. L. Blogg for preparation and analysis of samples, and of J. W. Simmons for editorial review of this report.

REFERENCES

1. R. K. Steunenberg, R. D. Pierce, and I. Johnson, "Status of the Salt Transport Process for Fast Breeder Reactor Fuels," Symposium Reprocessing of Nuclear Fuels, Ames, Iowa, Aug. 25-27, 1969, Nuclear Metallurgy, Vol. 15, USAEC Report CONF-690801 (1969), pp. 325-335.

2. T. R. Johnson, R. D. Pierce, F. G. Teats, and E. F. Johnston, Behavior of Countercurrent Liquid-Liquid Columns with a Liquid Metal, AIChE J. 17, 14-18 (Jan. 1971).

3. V. S. Morello and N. Poffenberger, Commercial Extraction Equipment, Ind. Eng. Chem. 42, 1021-1035 (1950).

4. R. B. Akell, Extraction Equipment Available in the U.S., Chem. Eng. Progr. 62, 50-55 (1966).

5. M. Benedict and T. H. Pigford, Nuclear Chemical Engineering, 1st ed., pp. 237-250, McGraw-Hill, New York (1957).

6. B. V. Coplan, J. K. Davidson, and E. L. Zebroski, The "Pump-Mix" Mixer-Settler, a New Liquid-Liquid Extractor, Chem. Eng. Progr. 50, 403-408 (1954).

7. E. R. Graef and S. P. Foster, Design of Box-Type Countercurrent Mixer-Settler Units - Factors Affecting Capacity, Chem. Eng. Progr. 52, 293-298 (1956).

8. J. H. Holmes and A. C. Schafer, Some Operating Characteristics of the Pump-Mix Mixer-Settler, Chem. Eng. Prog. 52, 201-204 (1956).

9. T. R. Johnson, F. G. Teats, and R. D. Pierce, An Induction Probe for Measuring Levels in Liquid Metals, Nucl. Appl. 4, 47-53 (1968).

10. D. R. Armstrong and R. D. Pierce, "Power Requirements for Mixing Liquid Metals," Chemical Engineering Division Summary Report, July, August, September 1962, ANL-6596, pp. 84-87 (1962).

11. R. E. Treybal, Liquid Extraction, 2nd ed., pp. 423-430, McGraw-Hill, New York (1963).

12. J. B. Knighton, I. Johnson, and R. K. Steunenberg, "Uranium and Plutonium Purification by the Salt Transport Method," Symposium on Processing of Nuclear Fuels, Ames, Iowa, Aug. 25-27, 1969, Nuclear Metallurgy, Vol. 15, USAEC Report CONF-690801 (1969), pp. 337-362.

13. W. J. Walsh, "Process Flowsheet Development," Chemical Engineering Division Annual Report, 1968, ANL-7575, pp. 28-29 (1969).